20th Conference on Climate Variability and Change New Orleans, LA January 2008
22nd Conference on Hydrology
J6.4

A preliminary study of global water and energy cycles in a NASA reanalysis system

Junye Chen[1,2] and Michael G. Bosilovich[2]
[1]*ESSIC, University of Maryland;* [2]*GMAO, GSFC NASA*

1 INTRODUCTION

Global water and energy cycles are two tightly related and critical components of the Earth climate system. In current assimilation systems, biased model output is only locally modified by the afterward analysis process based on available observations, which are always uncompleted and contaminated by random error and biases. Thus the global water and energy balances are good yet high standard indicators of the performance of an assimilation system. In this study, we use several global observed datasets to evaluate the assimilation results from the validation experiments for the Modern Era Retrospective-analysis for Research and Applications (MERRA) based on NASA GEOS-5 data assimilation system. The observed datasets include CERES ERBE-like radiation fluxes at the top of atmosphere (TOA), GPCP precipitation, CMAP precipitation etc. Furthermore, based on comparison with other assimilation systems, deeper understanding about the effect of the interaction between model and analyzed data on the water and energy cycles will be given.

2 DATA SETS

2.1 Global TOA radiation fluxes and precipitation observations

The Clouds and the Earth's Radiant Energy System (CERES) ERBE-like TOA radiation fluxes data (Wielicki et al., 1995, 1996, 1998), from two spaceships, Terra and Aqua, provide independent reference of TOA radiation fluxes. The difference between the data from the two satellites gave a measurement for the uncertainty of the observation.

The Global Precipitation Climatology Project (GPCP) version 2 monthly precipitation analysis (Huffman et al., 1997; Adler et al., 2003) and the CPC Merged Analysis of Precipitation (CMAP) (Xie and Arkin 1997) datasets are used as the baseline to compare with the precipitation output from reanalyses. GPCP and CMAP are both merged datasets based on rain gauge observations and satellite retrievals. They are not identical because difference in the input data and merge methods. The difference between these two datasets can be used as a rough measurement of the uncertainty of global long term precipitation observation.

2.2 MERRA

The Modern Era Retrospective-analysis for Research and Applications (official site: http://gmao.gsfc.nasa.gov/research/merra/ , data: http://disc.sci.gsfc.nasa.gov/MDISC/ , blog: http://merra-reanalysis.blogspot.com/) is a reanalysis project based on a new version of the Goddard Earth Observing System Atmospheric Data Assimilation System (GEOS-5). The MERRA time period will cover the modern era of remotely sensed data, from 1979 through the present, with a model and analysis resolution of 1/3 by 1/2 degrees and 72 levels extending to 0.01 hPa. The hydrological cycle is specially emphasized in MERRA. The water cycle benefits as unrealistic spin down is minimized by applying Incremental Analysis Updates (IAU) to slowly adjust the model states toward the observed state. Along with the Catchment hydrology land surface model, MERRA is anticipated to improve upon the representation of the water cycle in reanalyses.

In this study, we use monthly data from four segments of MERRA runs: August 1987, August 1987 without SSM/I data assimilated, January-July 2004, January-July 2006. The period of Jan-Jul 2004 gets more appearance here, but the associated conclusion does not lose generality.

2.3 Other long term global reanalyses

Data from four published global long term reanalyses are also analyzed in this paper. The four reanalyses are NCEP/NCAR Reanalysis 1 (NCEP1) (kalnay et al., 1996), NCEP-DOE AMIP-II Reanalysis (NCEP2) (Kanamitsu et al., 2002),

* *Corresponding Author Address*: Junye Chen, Global Modeling and Assimilation Office, NASA GSFC Code 610.1, Greenbelt, MD 20771 email: jchen@gmao.gsfc.nasa.gov

ECMWF 40 Year Re-analysis (ERA-40) (Uppala et al, 2005) and Japanese 25-year Reanalysis (JRA-25). ECMWF operational analysis data, which is considered as the best assimilation product, is also included when available.

3 ANALYSIS

3.1 Analysis over spatial domain

In both January and July 2004, all reanalyses data have positive mean biases from a few to around 15 W/m^2 in TOA LW flux, except NCEP/NCAR with a near neutral negative bias (Table 1). The standard deviations of the differences between reanalyses and CERES observation are comparable or larger than the mean biases (Table 1), implying strong variability in regional biases. As shown in Figure 1, the tropical region is where the strongest error happens for all reanalyses, especially over convection regions, at where the biases can reach 40 W/m^2. The regional biases in TOA SW flux are doubled in comparison with LW flux (Table 2). Seems this can be attributed to the extensive strong positive biases in the zonal band around 60°S, in addition to the biases happen over the tropical region(Figure 2).

The mean biases in precipitation are several times larger in ECOPS (~0.5mm/day), JRA25 (~0.7mm/day) and NCEP2 (~0.7mm/day) than in MERRA (~0.15mm/day) and NCEP1 (~0.2mm/day) (Table 3). These biases are considerable large, as the global mean precipitation is around 2.6mm/day based on GPCP and CMAP observation. As in TOA fluxes, the tropical region is where the strongest bias happens, and the middle latitude storm track regions are significant too.

Compared with other reanalyses, in the monthly fields, MERRA gives moderate result in TOA LW flux, relative better in TOA SW flux, and significant better result in precipitation, as shown in Table 1 – 3. In all three fields, the largest bias still locates over the tropical convective region. In the interannual time scale, the biases in MERRS are relative stable in spatial distribution for precipitation (Figure 4, right column), and other fields (not shown). At the same time, real interannual climate signal is well captured (Figure 4, bottom row).

3.2 The interrelationship between TOA fluxes and precipitation

TOA LW flux, SW flux and precipitation are tightly interrelated through cloud and water vapor. Here, we try to investigate and evaluate their interrelationship through joint frequency distribution (JFD, or joint histogram) of TOA SW and LW fluxes, and associated precipitation.

Figure 5 shows SW-LW JFDs based on global monthly data from January 2004 to July 2004. The JFD pattern from CERES (Figure 5, lower-left) gives a reference for the patterns based on reanalyses data. It is apparent that MERRA (GEOS5) pattern (Figure 5, lower-right) is more similar to the CERES pattern, while the distribution shape is a litter expanded. For comparison, the peaks of the distributions from NCEP2 (Figure 5, upper left) and JRA-25 (Figure 5, upper right) shift toward higher SW and LW condition, and lack the branch of the conditions of high SW flux and ~225W/m^2 LW flux.

The patterns of mean precipitation corresponding to SW-LW conditions are shown in Figure 6. In high SW and low LW condition, MERRA (Figure 6, lower right) shows extreme high precipitation not shown in the pattern based on observation (Figure 6, lower left), although the probability of these conditions is extremely low (Figure 5, lower right). Patterns from NCEP2 (Figure 6, upper left) and JRA-25 (Figure 6, upper right) have a systematic shift toward up-right side.

The patterns in Figure 7 are the products of the corresponding patterns in Figure 5 and Figure 6. They represent the precipitation distributions weighted by the frequency of occurrence of corresponding LW-SW conditions. Based on the observation data from CERES and GPCP, most of the precipitation happens in modest SW and LW condition (Figure 7, lower left). The pattern based on MERRA data (Figure 7, lower right) is much closer to the pattern based on observation, while a little bit stretched. This implies that LW, SW and precipitation are better integrated in MERRA system.

3.3 Global mean water and energy budgets

Because atmosphere itself is not a source of water and energy, its small water and energy storage capacity and the stability of the climate system, the global mean budget of water and energy at the upper and lower boundaries of the atmosphere should be roughly close to zero in annual time scale. This is not necessary the case

in a reanalysis system, since the state of the atmosphere is modified based on uncompleted observation and no global constrain on the global water and energy budget. In this section, we investigate the global budget of precipitation and evaporation, and the radiation energy budget at TOA, but not the surface energy budget because lack solid observation on surface fluxes.

In the global mean time series of the balance between precipitation and evaporation (Figure 8), only NCEP2 time series (orange line) keeps near zero in the whole time scope from 1984 to 2006. This is not strange, since no water vapor data from satellite is assimilated in the NCEP2 assimilation system, and this balance is the result of both higher precipitation and evaporation around 3.2mm/day, in comparison with observed global mean precipitation around 2.6mm/day from GPCP and CMAP (not shown). In all reanalyses, MERRA (Figure 8, red) is the only one keeps both a near observed global mean precipitation and a near balance between precipitation and evaporation in the 2000s. Although, P-E in the 1980s is unbalanced for about 0.2mm/day in MERRA, and the introduction of SSM/I data has a 0.1mm/day impact. The SSM/I impact in MERRA is less than those in JRA-25 (Figure 8, purple) and ERA-40 (Figure 8, blue).

At the top of atmosphere, the CERES observation shows an unbalance of ~5W/m^2 net downward radiation flux (Figure 11, light and dark brown lines). This unbalance mostly could be attributed to the missing boxes of SW flux observation in high latitudes around 70° (not shown). MERRA (red dot and lines) shows a good balance at TOA, especially during the 2000s, and the impact of SSM/I on TOA radiation flux balance is very small. Other reanalyses all show an unbalance around -10 W/m^2, this can be attributed to higher than observed TOA LW fluxes in JRA-25, and higher than observed TOA upward SW fluxes in NCEP2 and probably both in ERA-40 (Figure 9 and Figure 10).

4 CONCLUSION AND DISCUSSION

Compared with previous reanalyses, MERRA shows comparable or better results in global water and energy cycle. More room for improvement is still available, especially over tropical and subtropical region, storm track region, and south hemisphere high latitudes. Although the data in 1980s is very limited, it is apparent that the water and energy balance in 2000s is considerable better than that in 1980s in MERRA. This is understandable, since the tuning of GEOS5 system was concentrated on the 2000s, at when all modern observation systems are deployed, like EOS satellites.

In an assimilation system, after adjusted by analysis process based on observation, seems the model always tries to be back to its biased climatology, and then re-adjusted to near observation in the next analysis round. This charge and discharge spin-up (or down) loop apparently is one possible source of the questionable global energy and water budget in reanalyses. The application of IAU process in MERRA, may contribute to a better water and energy signals.

In a long term reanalysis system, when the observed data has one step significant change, an artificial discontinuity can be introduced in the reanalysis time series, as we showed in the comparison of 87run and 87run with out SSM/I. Multiple step changes in the observation system, as we experienced in recent decades, could result in multiple discontinuities, and cause artificial climate trend in the reanalysis data. This could be the reason of the big trend in P-E time series based on ERA-40 data.

ACKNOWLEDGEMENT

GPCP data provided by the Laboratory for Atmospheres, NASA Goddard Space Flight Center, from their web site at: http://precip.gsfc.nasa.gov/

CMAP data provide by the NOAA/NWS/CPC, from their web site at http://www.cpc.ncep.noaa.gov/products/global_precip/html/wpage.cmap.html

CERES ERBE-like data provided by NASA LARC, from their web site at http://eosweb.larc.nasa.gov/PRODOCS/ceres/table_ceres.html

NCEP/NCAR Reanalysis data provided by the NOAA/OAR/ESRL PSD, Boulder, Colorado, USA, from their Web site at http://www.cdc.noaa.gov/

NCEP-DOE_Reanalysis 2 data provided by the NOAA/OAR/ESRL PSD, Boulder, Colorado, USA, from their Web site at http://www.cdc.noaa.gov/

ERA-40 data provided by the European Centre for Medium-Range Weather Forecasts, from their web site at http://www.ecmwf.int/

JRA-25 data provided by the Japan Meteorological Agency (JMA) at their web site at http://jra.kishou.go.jp/index_en.html

REFERENCE:

Adler, R.F., G.J. Huffman, A. Chang, R. Ferraro, P. Xie, J. Janowiak, B. Rudolf, U. Schneider, S. Curtis, D. Bolvin, A. Gruber, J. Susskind, and P. Arkin, 2003: The Version 2 Global Precipitation Climatology Project (GPCP) Monthly Precipitation Analysis (1979-Present). J. Hydrometeor., 4,1147-1167.

Kalnay et al.,The NCEP/NCAR 40-year reanalysis project, Bull. Amer. Meteor. Soc., 77, 437-470, 1996.

NCEP-DEO AMIP-II Reanalysis (R-2): M. Kanamitsu, W. Ebisuzaki, J. Woollen, S-K Yang, J.J. Hnilo, M. Fiorino, and G. L. Potter. 1631-1643, Nov 2002, Bul. of the Atmos. Met. Soc.

Uppala, S.M., Kållberg, P.W., Simmons, A.J., Andrae, U., da Costa Bechtold, V., Fiorino, M., Gibson, J.K., Haseler, J., Hernandez, A., Kelly, G.A., Li, X., Onogi, K., Saarinen, S., Sokka, N., Allan, R.P., Andersson, E., Arpe, K., Balmaseda, M.A., Beljaars, A.C.M., van de Berg, L., Bidlot, J., Bormann, N., Caires, S., Chevallier, F., Dethof, A., Dragosavac, M., Fisher, M., Fuentes, M., Hagemann, S., Hólm, E., Hoskins, B.J., Isaksen, L., Janssen, P.A.E.M., Jenne, R., McNally, A.P., Mahfouf, J.-F., Morcrette, J.-J., Rayner, N.A., Saunders, R.W., Simon, P., Sterl, A., Trenberth, K.E., Untch, A., Vasiljevic, D., Viterbo, P., and Woollen, J. 2005: The ERA-40 re-analysis. Quart. J. R. Meteorol. Soc., 131, 2961-3012.doi:10.1256/qj.04.176

Huffman, G. J. and co-authors, 1997: The Global Precipitation Climatology Project (GPCP) combined data set. Bull. Amer. Meteor. Soc., 78, 5-20.

Wielicki, B.A., R.D. Cess, M.D. King, D.A. Randall, and E.F. Harrison, 1995: Mission to Planet Earth: Role of clouds and radiation in climate. Bull. Amer. Meteor. Soc., 76, 2125–2153.

Wielicki, B.A., B.R. Barkstrom, E.F. Harrison, R.B. Lee III, G.L. Smith, and J.E. Cooper, 1996: Clouds and the Earth's Radiant Energy System (CERES): An Earth Observing System experiment. Bull. Amer. Meteor. Soc., 77, 853–868.

Wielicki, B.A., and Coauthors, 1998: Clouds and the Earth's Radiant Energy System (CERES): Algorithm overview. IEEE Trans. Geosci. Remote Sens., 36, 1127–1141.

Xie P., and P. A. Arkin, 1996: Global precipitation: a 17-year monthly analysis based on gauge observations, satellite estimates, and numerical model outputs. Bull. Amer. Meteor. Soc., 78, 2539-2558.

TOA LW difference (W/m^2)	Jan, 2004		Jul, 2004	
	Ave	STD	Ave	STD
CERES Terra - Aqua	-0.8	2.4	-0.7	2.5
MERRA - CERES	5.4	9.1	2.5	12.8
ECOPS - CERES	8.9	7.3	7.6	6.8
JRA25 - CERES	16.2	9.0	15.8	10.3
NCEP1 - CERES	-0.5	11.4	-0.9	11.5
NCEP2 - CERES	4.6	14.4	4.1	14.4

Table 1. Average and standard deviation of monthly map of difference between TOA upward LW fluxes from different data sets.

TOA NET SW difference (W/m^2)	Jan, 2004		Jul, 2004	
	Ave	STD	Ave	STD
CERES Terra - Aqua	-1.7	9.3	0.6	6.1
MERRA - CERES	-3.2	17.2	-5.2	20.7
ECOPS - CERES	-2.6	16.7	-3.5	15.5
JRA25 - CERES	2.4	24.6	0.3	21.0
NCEP1 - CERES	-21.5	25.6	-18.1	23.5
NCEP2 - CERES	-7.9	29.8	-7.2	26.6

Table 2. Similar as table 1, except for TOA downward net SW flux.

Precip difference (mm/day)	Jan, 2004		Jul, 2004	
	Ave	STD	Ave	STD
GPCP - CMAP	0.0	0.9	0.1	0.9
MERRA - ave(GP,CM)	0.1	1.2	0.2	1.3
ECOPS - ave(GP,CM)	0.5	1.3	0.5	1.3
JRA25 - ave(GP,CM)	0.6	1.6	0.8	2.2
NCEP1 - ave(GP,CM)	0.1	1.6	0.3	1.7
NCEP2 - ave(GP,CM)	0.6	2.4	0.8	2.9

Table 3. Similar as table 1, except for precipitation.

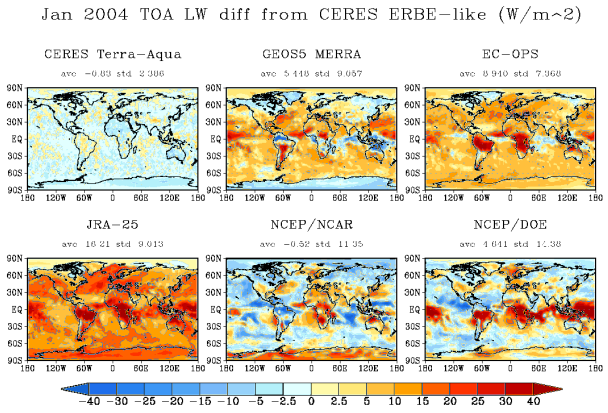

Figure 1. Monthly mean TOA Longwave flux difference spatial distributions in January 2004.

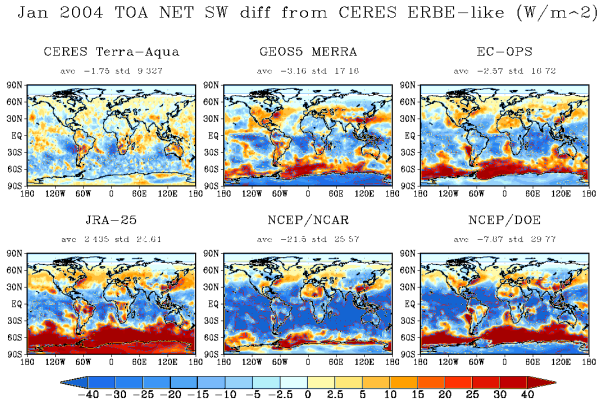

Figure 2. Similar as figure 1, except for TOA downward net SW flux.

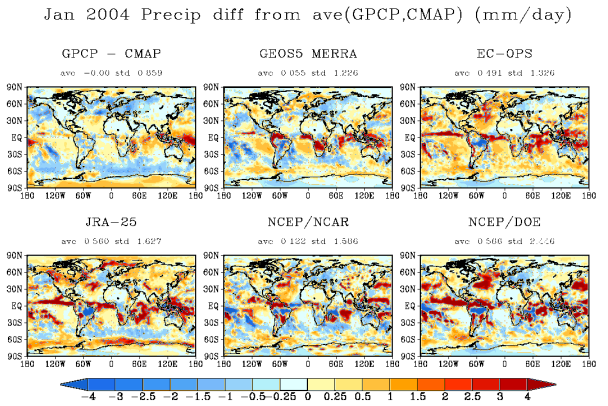

Figure 3. Similar as figure 1, except for precipitation.

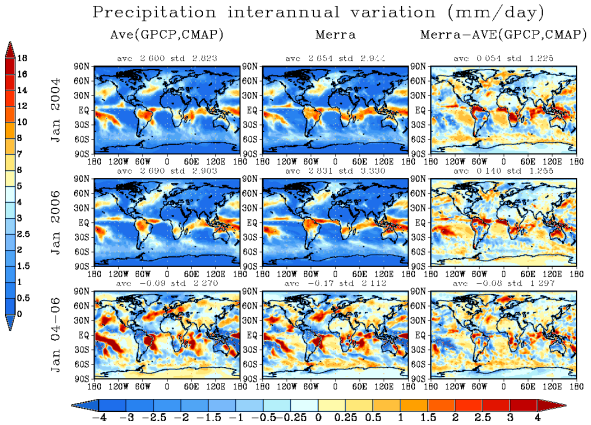

Figure 4. Precipitation interannual variation and difference between MERRA and the average of GPCP and CMAP.

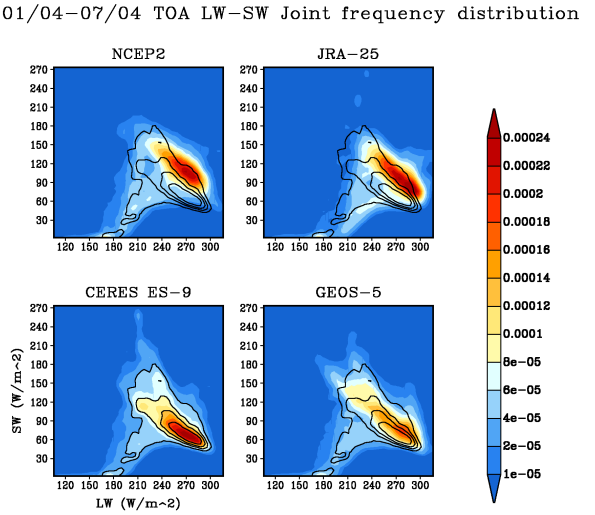

Figure 5. Global Joint frequency distribution of TOA LW and SW over the period from January 2004 to July 2004. The black contour in lower-left panel is duplicated to other three panels for easy comparison.

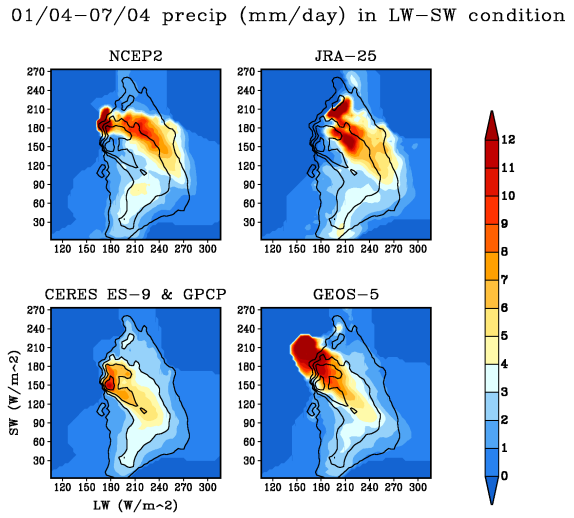

Figure 6. Mean precipitation corresponding to SW-LW conditions. The black contour in lower-left panel is duplicated to other three panel.

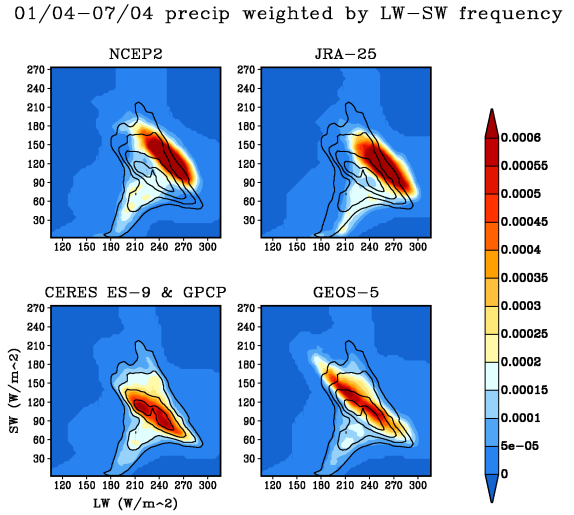

Figure 7. The product of figure 5 and figure 5. It represents the precipitation weighted by the frequency of occurrence of LW-SW conditions. The black contour in lower-left panel is duplicated to other three panel.

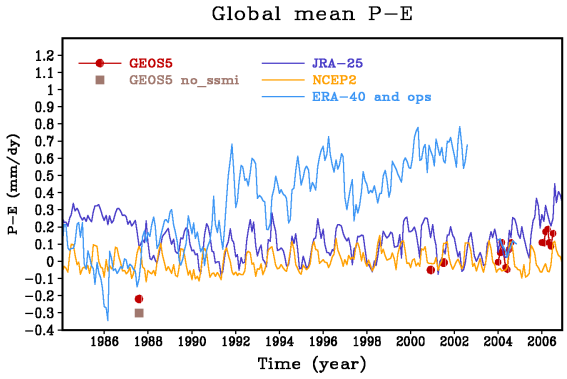

Figure 8. Global mean time series of precipitation minus evaporation from reanalyses.

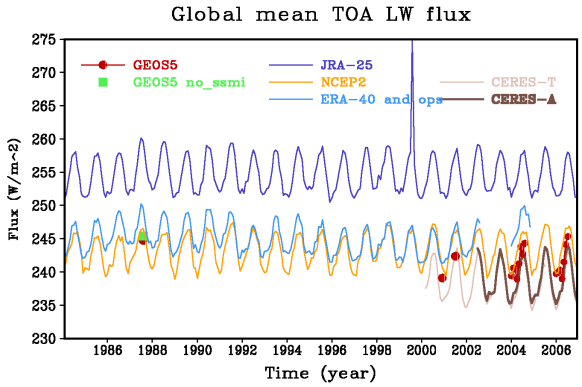

Figure 9. Global mean time series of upward LW fluxes at TOA.

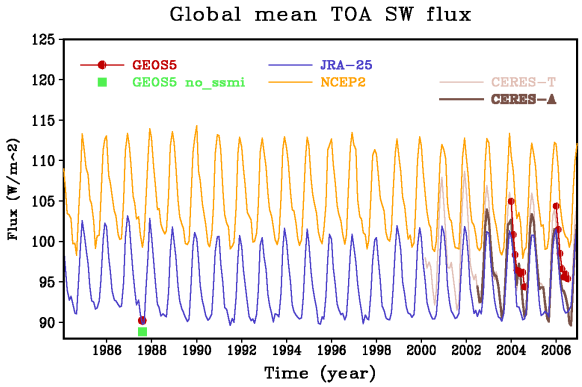

Figure 10. Global mean time series of upward SW fluxes at TOA.

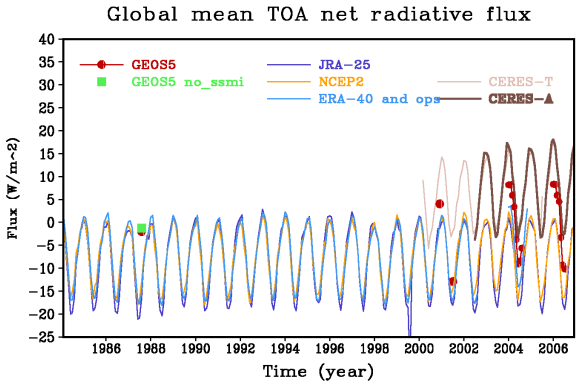

Figure 11. Global mean time series of net downward radiation fluxes at TOA.